BMC Microbiology

RESEARCH Open Access

Emergence of hypervirulent and carbapenem-resistant *Klebsiella pneumoniae* from 2014 - 2021 in Central and Eastern China: a molecular, biological, and epidemiological study

Chunyang Wu[1], Yu Huang[2], Peiyao Zhou[3], Haojin Gao[3], Bingjie Wang[3], Huilin Zhao[3], Jiao Zhang[3], Liangxing Wang[4*], Ying Zhou[3*] and Fangyou Yu[2,3*]

Abstract

Background In recent years, the hypervirulent and carbapenem-resistant *Klebsiella pneumoniae* has been increasingly reported worldwide. The objective of this study was to compare the antibiotic resistance and virulence profiles of carbapenem-resistant hypervirulent *K.pneumoniae* (CR-hvKP) and hypervirulent carbapenem-resistant *K.pneumoniae* (hv-CRKP) and identify the prevailing strain in clinical settings.

Methods In this study, hv-CRKP or CR-hvKP were identified based on the results of whole-genome analysis (WGS), multilocus sequence typing (MLST) and the antimicrobial susceptibility testing. We then compared antibiotic resistance and virulence profiles between CR-hvKP and hv-CRKP through the antimicrobial susceptibility testing and a series of virulence experiments including biofilm formation ability detection method, the resistance test against human serum, siderophore production test, neutrophil phagocytosis assay and *Galleria mellonella* infection model. Additionally, pathway enrichment analysis was conducted to assess the effect of SNPs on the phenotype.

Results In this study, we categorized 17.4% of hypervirulent and carbapenem-resistant *K. pneumoniae* strains as CR-hvKP and 82.6% as hv-CRKP. Among them, 84.2% (16/19) of CR-hvKP strains harboring carbapenemase genes exhibited lower imipenem and meropenem MIC values compared to hv-CRKP strains. The virulence potential of hv-CRKP and CR-hvKP was confirmed by using virulence experiments in vitro and in vivo, showing that virulence of the CR-hvKP strains was comparable to that of hv-CRKP strains. Notably, the 90 hv-CRKP strains were classified into 3 different ST types and 8 capsule types, each showing varying degrees of resistance and virulence. We observed that

*Correspondence:
Liangxing Wang
wangliangxing@wzhospital.cn
Ying Zhou
18702195157@163.com
Fangyou Yu
wzjxyfy@163.com

Full list of author information is available at the end of the article

subclonal replacement was within the predominant hv-CRKP clone, with the ST11-KL64 strain, characterized by high-level resistance and virulence emerging as the currently prevailing subclone, replacing ST11-KL47. KEGG enrichment analysis showed that pathways associated with the citrate cycle (TCA cycle), glycolysis/gluconeogenesis, glutathione metabolism, two-component regulatory system, and folate metabolism were significantly enriched among the group expressing different levels of capsular polysaccharides.

Conclusions The hv-CRKP strains exhibited a greater survival advantage in the hospital environment than CR-hvKP strains. Notably, the ST11-KL64 hv-CRKP strain which displayed a high level of resistance and hypervirulence, warrants the most clinical vigilance.

Clinical trial number Not applicable.

Keywords Hypervirulent, Carbapenem-resistant, *Klebsiella pneumoniae*, ST11-KL64

Introduction

Carbapenem-resistant *Klebsiella pneumoniae* (CRKP) is classified as a critical threat by the World Health Organization (WHO) due to its high dissemination, mortality, and limited treatment options [1]. Hypervirulent *K.pneumoniae* (hvKP), which first emerged in Taiwan, China in the 1980s, has acquired virulence determinants making it more pathogenic than the classical *K. pneumoniae* (cKp)[2]. Recently, the ongoing evolution of plasmids carrying genes for hypervirulence or carbapenem resistance has led to the emergence of hypervirulent and carbapenem-resistant *K. pneumoniae* [3]. This evolution has been observed to follow three distinct pathways. One pathway involved the acquisition of a carbapenem-resistance plasmid by certain hypervirulent *K.pneumoniae* strains, such as KL1/KL2 hvKP, resulting in carbapenem-resistant hypervirulent *K.pneumoniae* (CR-hvKP) [4]. Another evolutionary pathway involved the acquisition of virulence plasmids by non-K1/K2 CRKP, such as ST11/ST258, leading to the emergence of hypervirulent CRKP (hv-CRKP) [5, 6]. The widespread occurrence of conjugative helper plasmids encoding carbapenemase, such as bla_{KPC-2} and bla_{NDM-1}, along with the presence of the conserved *oriT* in virulence plasmids, may facilitate these evolutionary processes. In addition to acquiring transmissible resistant plasmids, hvKP isolates also demonstrate the ability to integrate resistance genes into their own virulence plasmids. For example, the plasmid pKP70-2 was inserted into a bla_{KPC-2}-encoding region flanked by two copies of IS26[7]. The most common type of clinical infection caused by hypervirulent and carbapenem-resistant *K. pneumoniae* is caused by CR-hvKP and hv-CRKP strains. In recent years, the emergence of CR-hvKP and hv-CRKP has spurred numerous studies and attracted significant global attention [8, 9]. However, the majority of research has not characterized the molecular epidemiology, virulence, and resistance profiles of these two patterns of evolution of *K. pneumoniae* in detail.

In this study, we collected 109 hypervirulent and carbapenem-resistant isolates of *K. pneumoniae* from 11 hospitals in central and eastern China over an 8-year period from 2014 to 2021 for analysis. The 109 isolates were divided into two classes (CR-hvKP and hv-CRKP) based on the evolutionary path of the acquisition of carbapenem resistance and hypervirulence genes.

We used in vitro and in vivo virulence assessment experiments and antimicrobial susceptibility testing to compare the antibiotic-resistant and hypervirulent phenotypes between CR-hvKP and hv-CRKP. Additionally, we applied whole-genome sequencing (WGS) to analyze the molecular mechanisms associated with the hypervirulent and multidrug resistance phenotypes. Furthermore, we combined single nucleotide polymorphism (SNP) and functional analyses to investigate the differences of function between the bacterial taxa and the possible mechanism behind their abnormal functions.

ST11, previously identified as cKp, previously presents with lower virulence. Recently, a fatal outbreak of ST11 carbapenem-resistant hypervirulent *K. pneumoniae* in a Chinese hospital has raised concerns [8]. These isolates pose a substantial threat to human health as they are simultaneously hypervirulent, multidrug resistant, and highly transmissible. Notably, ST11 has evolved into two distinct clades: CR-hvKP presenting with KL64 and CR-cKp associated with KL47, both of which have been circulating in parallel within the hospital and healthcare institute. Previous studies of our team have reported a comparison of ST11-KL64 hv-CRKP and KL1/KL2 CR-hvKP, which had high pathogenicity, were fast transmissible, and multidrug-resistant, in a Chinese hospital [10]. However, few studies have focused on the epidemiological characteristics of ST11-KL64 hv-CRKP isolates. In this study, we will meticulously describe the prevalence and evolutionary characteristics of ST11-KL64 hv-CRKP isolates. According to our study, hv-CRKP poses a substantial threat to the health care, and urgent measures are required to monitor and control the spread of these hyper-resistant and hypervirulent superbugs.

Materials and methods

Bacterial isolates

A total of 207 non-duplicate CRKP isolates were collected from different clinical specimens of patients admitted to 11 teaching hospitals in central and eastern China. All isolates were verified as *K. pneumoniae* by MALDI-TOF and tested for antibiotic susceptibility with the VITEK2 system. CRKP was defined as resistance to at least one carbapenem antibiotic. All isolates were preserved in broth with 40% glycerol and stored at −80 ℃.

Whole-genome sequencing and analyses

Bacterial DNA was extracted using the DNA extraction kit (TIANGEN, Beijing) following the manufacturer's instructions. Sequencing libraries were generated with the NEBNext® Ultra™ DNA Library Prep Kit for Illumina® (NEB, USA). Then, preliminary quantification was performed with Qubit2.0 and the insert size of the library was detected using Agilent 2100. After qualification, Illumina HiSeq/MiSeq sequencing was performed by pooling different libraries according to the required effective concentration and target data amount. We used the online tool Reference sequence Alignment for SNP analysis and constructed a phylogenetic tree based on SNPs, using FK3009 (ST11-KL64 hv-CRKP) as a reference. Evolview v3 was used to visualize and beautify the phylogenetic tree. Several SNP annotation databases were used to identify possible SNP functions. Isolates were categorized into two groups based on the level of expression of four distinct phenotypic characteristics: capsular polysaccharide production, siderophore production, biofilm formation, and resistance to meropenem. To determine the variation among groups, the frequency of each allele was calculated for each SNP and compared between the two groups. Pathway analysis was performed using KEGG Automatic Annotation Server (KAAS) (http://www.genome.jp/tools/kaas/) and clusterProfiler (Version 4.6.2). Statistical analyses were conducted in R (R version 3.4.4).

Antimicrobial susceptibility testing

The antimicrobial susceptibility of the isolates was determined using standard broth microdilution method, following to the Clinical and Laboratory Standards Institute guidelines (CLSI, 2022). We used *Escherichia coli* ATCC 25922 as the quality control organism for MIC determination. The breakpoints for colistin and tigecycline were based on European Committee on Antimicrobial Susceptibility Testing (EUCAST, 2022) guidelines. Each AST was independently repeated three times in our study.

The biofilm quantification assay

The biofilm formation ability was detected using the crystalline violet staining method, as described elsewhere in the literature, with minor modifications. After fixing the biofilm with anhydrous for alcohol 20 min and staining with 0.1% (wt/vol) crystal violet for 10 min, 200 μL of absolute ethanol was added to dissolve the biofilm for the quantitative assay. The optical density (OD595) was measured to quantify biofilm production.

Quantitative siderophore production assay

To assess the iron-chelating capabilities of bacterial supernatants, the chrome azurol S (CAS) assay was performed following established protocols. Specifically, bacterial clones (1 μL) were dropped on CAS and King's B agar plates prepared in a 2:1 ratio, and the presence of orange halos around the clones was used to identify siderophore production.

Capsular polysaccharide quantification assay

Bacteria (0.5 mL, OD = 1.0) were mixed with 100μL of 1% Z wittergent 3–14 detergent at 50℃ for 20 min, followed by centrifugation to obtain the supernatant. Then 300μL of supernatant was taken and mix with 1.2mL of ethanol for 20 min on ice to precipitate the capsular components. Subsequently, a sodium tetraborate solution in concentrated sulfuric acid (12.5 mM) was added, and the uronic acid content of the polysaccharides was determined using the m-hydroxybiphenyl method to measure uronic acid.

Serum killing assay

Briefly, prior to the assay, the serum separated from venous blood samples was stored at −80 °C. An inoculum of ~ 1×10^6 CFU bacteria in 25 μL, prepared from the mid-log phase, was mixed with 75 μL human serum. The mixture was incubated at 37 °C for 3 h, and after appropriate dilution at different time points (1 h, 2 h, and 3 h), it was spread-plated on MHA plates. The plates were incubated at 37℃ for 24 h and the number of colonies was counted. The rate of serum resistance was determined as the ratio of the number of colonies to the initial number of seeded colonies for each time. The survival ratio was calculated; all values of ≥ 40% at each time point were defined as indicative of serum resistance.

Neutrophil phagocytosis assay

Human neutrophils were isolated using a neutrophil isolation kit, following the manufacturer's protocol. The FITC-labeled *K. pneumoniae* was incubated with neutrophils at a ratio 5:1 at room temperature in the dark for 40 min. The cell suspension was collected at 10 min, 20 min, 30 min and 40 min points. The fluorescence of FITC was detected by flow cytometry using a BD flow Cytometer. Phagocytic activity (PA) = (Number of neutrophils involved in phagocytosis/all neutrophils) × 100%.

*Galleria mellonella*infection model studies

We stored the caterpillars of *G.mellonella* at 4 °C and in darkness before use to ensure their fitness and health. The caterpillars selected for the experiments weighed 200–250 mg each. They were injected at the left proleg with 10 μL (~1×10^6 CFU) bacterial suspension, while the control groups were injected with PBS or an empty syringe. The total number of caterpillars in each group was 10, and they were kept in culture at 37 °C and inspected for 144 h. The survival rates of each group were recorded for each day.

Statistical analysis

GraphPad prism 8 software (GraphPad Software) was used for statistical analysis. Continuous variables were compared using independent-group Student's t tests or the Mann–Whitney U tests. For in vivo and vitro experiments survival data were analyzed by the Log Rank test (Mantel-Cox).

Results

hv-CRKP isolates were more prevalent than CR-hvKp isolates in China

Between 2014 and 2021, 207 CRKP isolates were collected from 11 tertiary teaching hospitals across 9 provinces in China (Fig. 1A). *K. pneumoniae* isolates were divided as hvKP and non-hvKP based on the presence of any one of the virulence genes, including *rmpA*, *rmpA2*, *iucA* and *iroN*. CRKP isolates were further categorized into CR-hvKP and hv-CRKP based on their evolutionary path regarding the acquisition of carbapenem resistance and hypervirulence genes. We identified 98 other CRKP and 109 hypervirulent and carbapenem-resistant isolates including 90 hv-CRKP and 19 CR-hvKP (Fig. 1B). Within the hv-CRKP isolates, we identified five sequence types (STs), with ST11 (72/90; 84.4%) being the most prevalent, followed by ST15 (7/90; 7.8%) and ST290 (7/90; 7.8%) (Fig. 1C). The proportion of ST11-KL64 increased from 43.5% (27/62) in 2014 to 74.7% (77/103) in 2020,

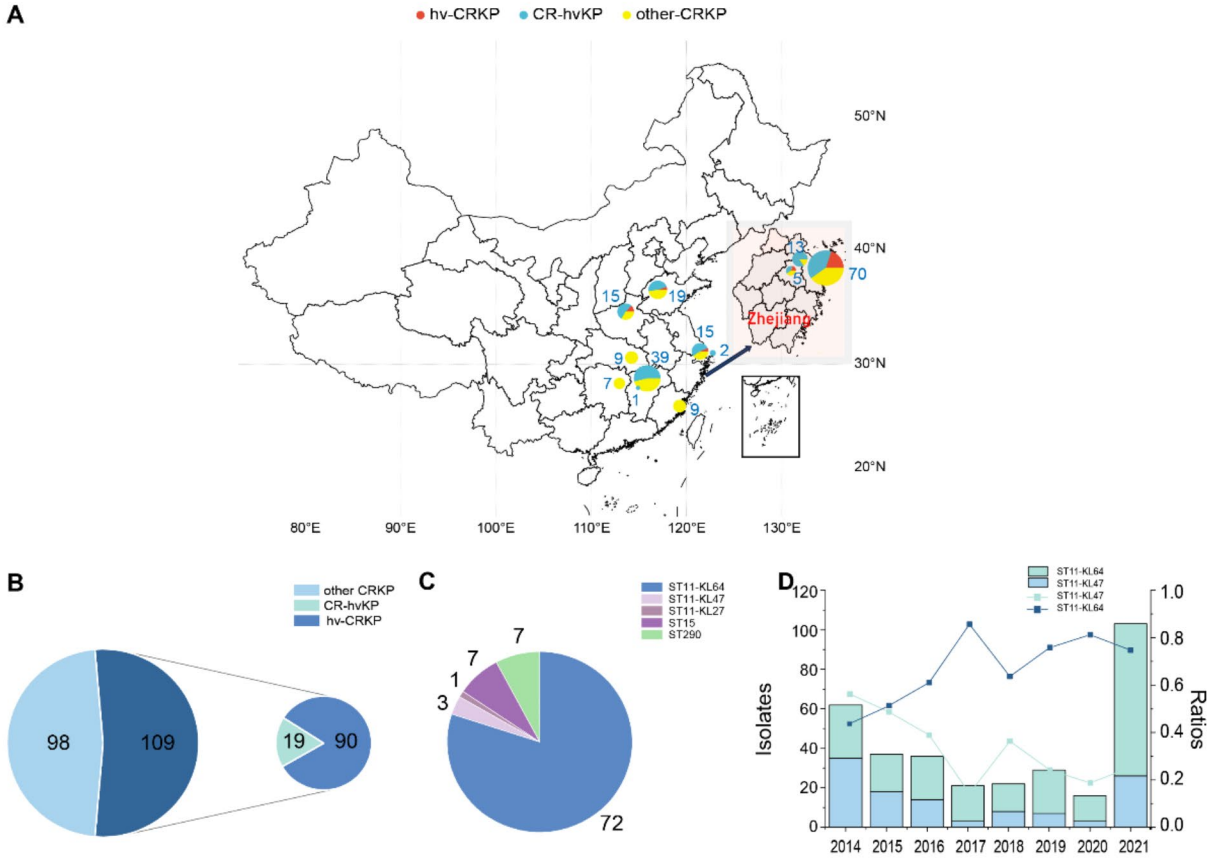

Fig. 1 Distribution of *K. pneumoniae* isolates collected in this study between 2014 and 2021 **A** Geographical distribution of 207 CRKP isolates participating in this study. Different colors represent different types of CRKP. **B** Proportion of CR-hvKP and hv-CRKP in CRKP. **C** The distribution of STs of 109 hypervirulent and carbapenem-resistant *K. pneumoniae*. **D** The graph shows the number of KL64 and KL47 detected in CRKP (bule bars) each year, and the ratio of KL64 to CRKP-ST11 (wathet blue line) and KL47 to CRKP-ST11(blue line)

while the proportion of ST11-KL47 among ST11-CRKP decreased from 56.4% (35/62) in 2014 to 25.2% (26/103) in 2020 (Fig. 1D). Further analysis of the line graph demonstrated that subclonal replacement has occurred from KL47 to KL64 within the ST11 population in 2015.

In terms of inpatient ward distribution of hypervirulent and carbapenem-resistant isolates, the majority of ST11-KL64 were isolated from emergency ICU (41.4%), surgery and other departments (10.5%), while most CR-hvKP analyzed were isolated from ICU (Fig. 2A). ST290 and ST11-KL47 isolates (100%) were exclusively isolated from surgery and other departments. CR-hvKP (12/19, 63.2%) and hv-CRKP(60/90, 66.7%) were recovered mainly from blood (Fig. 2B). The majority of isolates in ST11-KL64, K1/K2 and other CR-hvKP groups were isolated from blood, while ST15 isolates were obtained from blood and sputum. Based on the collection year, CR-hvKP were predominantly collected in the years-2020. However, ST11-KL64 hv-CRKP circulated at a low level prior to 2015 and remained persistently prevalent during 2015 to 2021 (Fig. 2C). ST290 was mainly collected in 2016 and 2017, after which they gradually disappeared. The ST15 and ST11-KL47 mainly concentrated after 2017.

Comparison of virulence and resistance phenotype in the CR-hvKP and hv-CRKP isolates

To clarify the antibiotic-resistant phenotype of these CR-hvKP and hv-CRKP isolates, each strain was tested the susceptibility to 17 antibiotics (Fig. 3E). We found that CR-hvKP was resistant to multiple antibiotic classes, with most isolates showing resistance to all β-lactam antibiotics and carbapenems. Over 36% of other CR-hvKP isolates were resistant to tigecycline, minocycline, ciprofloxacin and cotrimoxazole, however, the resistance ratio of KL1/KL2 CR-hvKP was not as high as that of other CR-hvKP isolates. The resistance rate of other CR-hvKP was 29% for gentamicin and amikacin, with no evidence of gentamicin and amikacin resistance observed among KL1/KL2 CR-hvKP. Results of antibiotic resistance in 90 hv-CRKP isolates showed that antibiotic susceptibility profiles of hv-CRKP were similar to those of CRKP, with high resistance to all β-lactam antibiotics and carbapenems observable. ST11 and ST15 hv-CRKP showed similar high resistance to tigecycline, amikacin, ciprofloxacin, and gentamicin, while ST290 results showed susceptibility or intermediate susceptibility to most of the antibiotics tested. Among 109 isolates, resistance rates to ceftazidime-avibactam of KL1/KL2 CR-hvKP and ST11-KL64 hv-CRKP were 40% and 10%, respectively. Polymyxin-resistant isolates were detected in ST11-KL64 hv-CRKP and other CR-hvKP, although no *mcr* -genes were detected.

To evaluate the virulence level of CR-hvKP and hv-CRKP isolates, we conducted a series of virulence related phenotypes experiments. Among the five KL1/KL2 CR-hvKP isolates, the string test was positive for all, with each producing strings longer than 20 mm. The string test positive rate among the 14 other CR-hvKP isolates was 5/14 (35.7%) (Fig. 3A). For ST11-KL64 hv-CRKP isolates, the positive rate was 34/72 (47.2%), while ST11-KL47, ST11-KL27, ST15 and ST290 all produced negative string test results. As shown in Fig. 3B, all KL1/KL2 CR-hvKP and ST290 hv-CRKP isolates had an average survival of 40% after incubation with the human serum for 180 min. However, the positive rate of other hv-CRKP differed from that of KL1/KL2 CR-hvKP, with only 14% (2/14) having an average survival rate of 40%, which was lower than that of ST11-KL64 hv-CRKP isolates (50%). Biofilm-forming capacity was assessed in all isolates. ST11-KL64 isolates produced significantly less biofilm than CR-hvKP isolates, but the biofilm-forming ability varied greatly among isolates tested ($P<0.05$) (Fig. 3C,

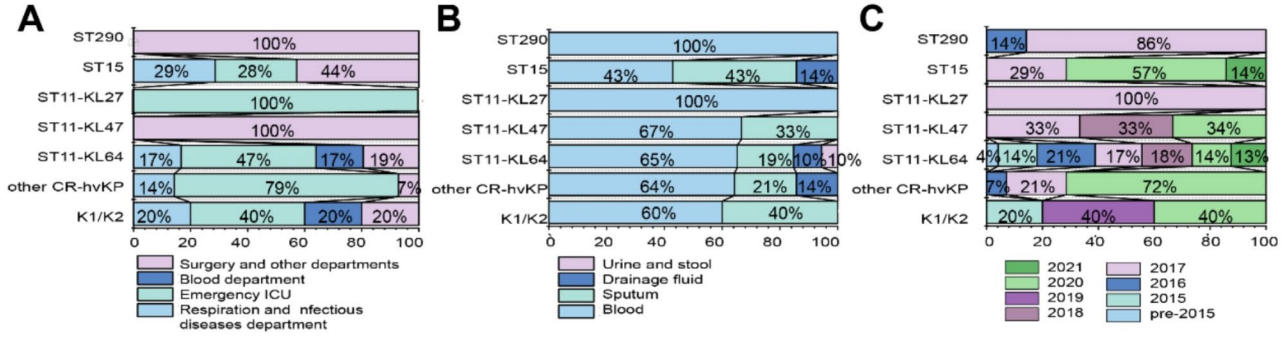

Fig. 2 Demographic characteristics and clinical features of 109 hypervirulent and carbapenem-resistant *K. pneumoniae***A** The department of these bacteria are available in Fig **A**, other departments includes an assortment of departments that were grouped because the numbers of patients admitted to each department were too small to display separately. Different colors represent different clinical departments. **B** The bacteria were obtained from different specimens. Different colors represent different specimens. **C** Proportion of different species isolated in different years. Different colors represent different years

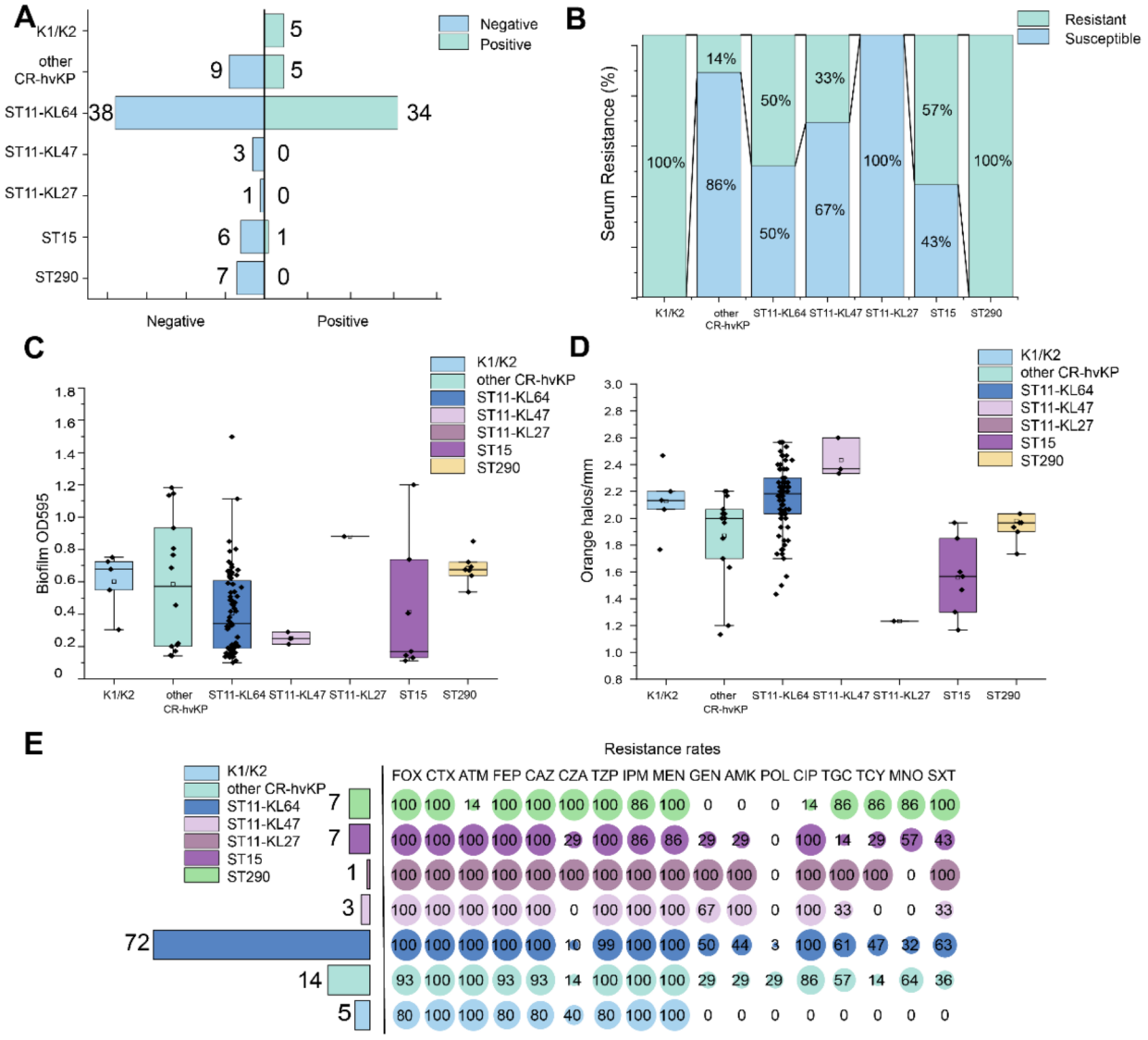

Fig. 3 The virulence and resistance phenotypes and levels between hv-CRKP and CR-hvKP. **A** The strips in the string test counted > 5 mm were defined to be positive, while ≤ 5 mm were defined to be negative. **B** Results from serum resistance assays. The survival of isolates after 1 h, 2 h and 3 h of incubation with serum greater than 40% was defined as serum resistance. **C** Biofilm formation capability of hv-CRKP and CR-hvKP, the values were measured at OD595 **D** Siderophores production determined by CAS agar plate of hv-CRKP and CR-hvKP. Yellow halos around bacterial colonies indicate siderophore. **E** Drug resistance rates of strain in different groups to 17 antimicrobial drugs. The number of strains was shown in each bar. The circle sizes indicate the percentage of strains exhibiting resistance to the antimicrobial drugs. FOX, cefoxitin; CTX, cefotaxime; ATM, aztreonam; FEP, cefepime; CAZ, ceftazidime; CZA, ceftazidime-avibactam; TZP, piperacillin-tazobactam; IPM, imipenem; MEN, meropenem; GEN, gentamicin; AMK, amikacin. POL, polymyxin B; CIP, ciprofloxacin; TGC, tigecycline; TCY, tetracycline; MNO, minocycline; SXT, sulfamethoxazole

Fig S1A). Quantitative siderophore assays indicated that except the ST15 hv-CRKP isolates, which displayed marked individual variability, all hv-CRKP produced comparable siderophores to CR-hvKP ($P>0.05$), and the ST11-KL64 hv-CRKP were more advantageous in siderophores production compares to other hv-CRKP ($P<0.05$) (Fig. 3D, Fig S1B).

Considering the strain sequence types and their serotypes, we selected 1390 (ST375-KL2), FK3128 (ST23-KL1), FK3062 (ST412-KL67), FK3009 (ST11-KL64), 1622 (ST11-KL64), FK3065 (ST11-KL47), 1050(ST111-KL27) and FK3006(ST15-KL112) with complete genome sequences in CR-hvKP and hv-CRKP for further virulence experiments, as they were highly representative and can provide more reliable results. All isolates formed capsular polysaccharide, and a trend towards higher capsular polysaccharide formation was observed for the KL1/KL2 CR-hvKP and ST11-KL64

hv-CRKP (Fig. 4E, Fig S1C). We used flow cytometry to examine fluorescent bacteria engulfed by neutrophils. We found that the phagocytosis of CR-hvKP by the neutrophils was similar to that of ST11-KL64 hv-CRKP, while the inhibition of phagocytosis of ST15 and ST290 was lower (Fig. 4AB). We further estimated pathogenicity using a *G.mellonella* larvae infection model with an inoculum of 1×10^6 CFU. The *G.mellonella* larvae infected with the CR-hvKP and ST11-KL64 hv-CRKP had a lower survival rate than those infected with the ST15, ST290 and other CR-hvKP isolates (Fig. 4D). The ST11-KL64 hv-CRKP isolates were more advantageous in the production of capsule polysaccharide, serum survival, biofilm, and siderophores, although some variability was observed among them.

hv-CRKP isolates contained virulence genes and antimicrobial resistance genes, with bla_{KPC-2} being the dominant type

We further characterized these 109 isolates for the presence of the resistance genes and the virulence genes (Fig. 5). We identified contigs associated with virulence based on the presence of the virulence associated genes *rmpA*, *rmpA2*, *iutA*, *iucABCD* and *iroBCDN* in *K. pneumoniae* genomes (Table S1). The results of virulence gene analysis indicated that *iutA*, *iucA* and *iucBCD* were commonly present in hv-CRKP, found in 97.3% (74/76), 97.3% (74/76) and 98.7% (75/76) of the isolates in the ST11 group, respectively. Additionally, 78.9% (60/76) of ST11 isolates harbored the combination of *iucA*+*rmpA*/*rmpA2*, in contrast, while 7 of 76 ST11 hv-CRKP isolates possessed *iroBCDN*. The positive rate of *iroBCDN* was significantly lower in ST11 hv-CRKP isolates compared

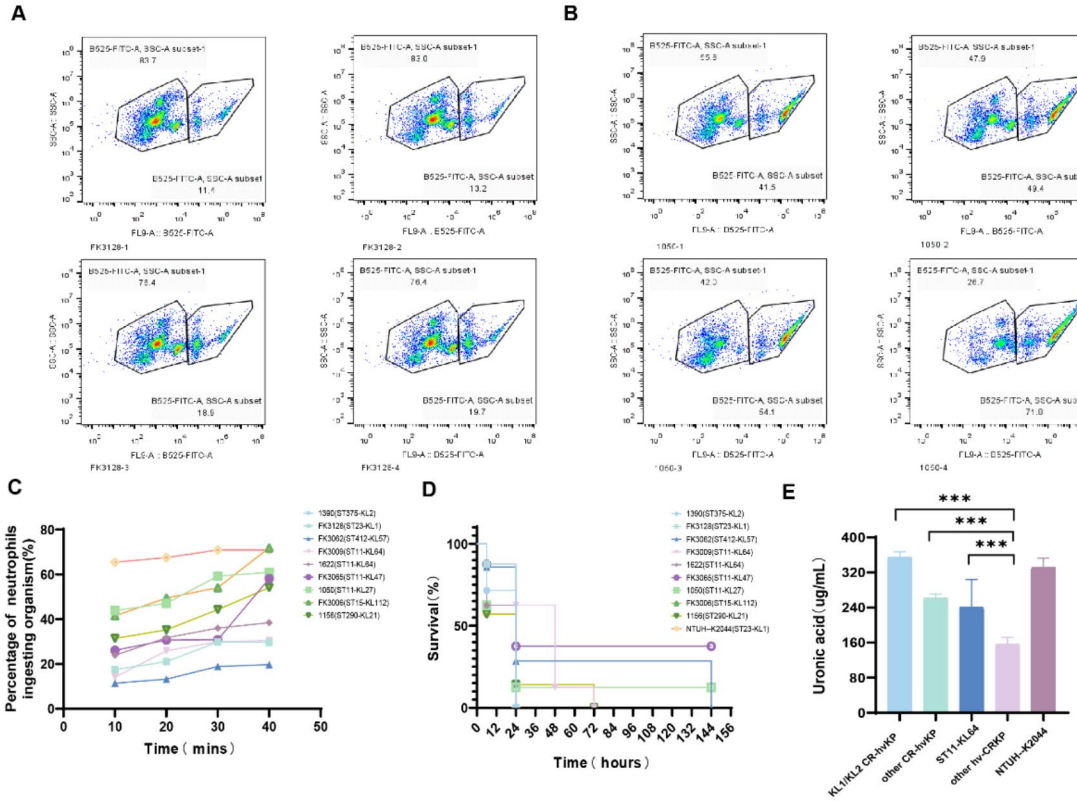

Fig. 4 The virulence and resistance phenotypes levels of representative strains. **AB** Flow cytometric plots. Neutrophil phagocytosis among CR-hvKP and hv-CRKP from wild-type isolates of serotype K1/K2 and ST11 with serotype KL47 isolates. The percent neutrophils with phagocytosed bacteria. Four different times, covering 10 min (1), 20 min (2), 30 min (3), and 40 min (4) were showed. **C** Neutrophil phagocytic capacity for representative strains Neutrophil phagocytic capacity percentage changes in response to acute exercise. The higher the percentage, the weaker virulence. **D** Survival rates of *G. mellonella* infected with representative strains, PBS, and none. Log-rank test was performed for analysis of the indicated curves. **E** Capsular polysaccharide quantification data. The uronic acid component of capsular polysaccharides from selected strains was estimated by using the sodium tetraborate reaction as an alternative chemical method to estimate capsule content. *$P<0.05$, ** $P<0.01$, *** $P<0.001$, ns: not significant

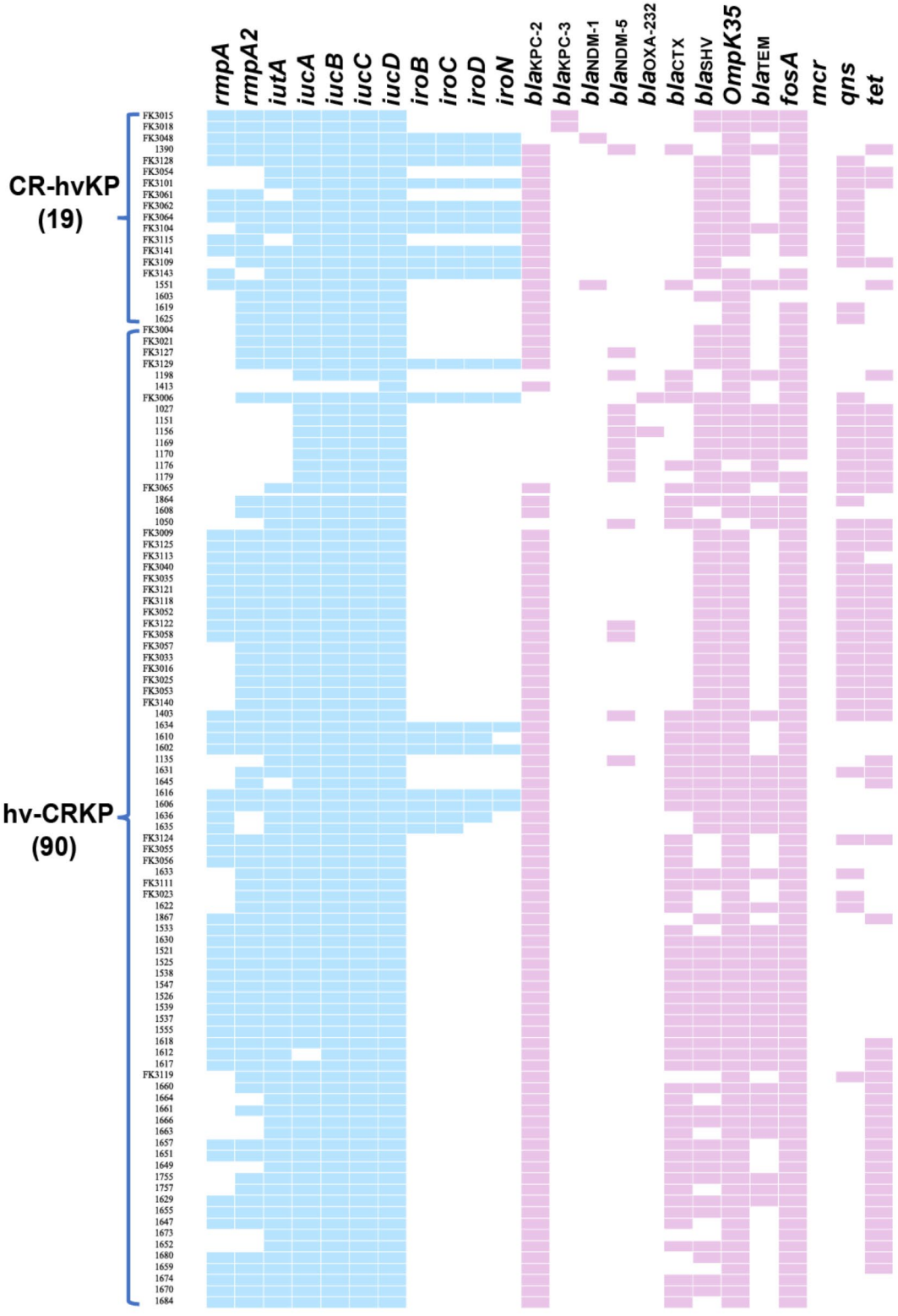

Fig. 5 Distribution of antibiotic resistance genes and virulence genes in 109 hypervirulent and carbapenem-resistant *K. pneumoniae*. 11 virulence genes and 13 resistance genes were determined by PCR. Colors represent genes of different categories

to CR-hvKP (10/20). The situation with virulence genes *iutA*, *iucABCD* and *iroBCDN* was similar for ST15 and ST290, 85.7% (6/7) of ST15 isolates possessed the *rmpA2* gene, whereas none of ST290 carried the *rmpA2* gene. We also detected the *rmpA2* gene in 85 isolates, among which isolates (15.3%) possessed truncated *rmpA2* genes, 61 isolates had an intact *rmpA2*, 10 isolates had indel mutations in *rmpA2*, and 3 isolates had a frameshift mutation in *rmpA2* (Table S2). These results showed that the expressions of hypervirulence-specific factors differed between hv-CRKP and CR-hvKP isolates, with CR-hvKP isolates carrying more virulence genes.

In this study, to further understand the differences in the distribution of antimicrobial resistance genes in CR-hvKP and hv-CRKP, we analyzed the 109 sequenced isolates for multi-resistance gene. A total of five types of carbapenemase genes were identified, including bla_{KPC-2} (88.1%, 96/109), bla_{KPC-3} (1.8%, 2/109), bla_{NDM-1} (1.8%, 2/109), bla_{NDM-5} (11.9%, 13/109), $bla_{OXA-232}$ (1.8%, 2/109). Screening for carbapenemase genes showed that all test isolates carried bla_{KPC} or bla_{NDM}. Two hv-CRKP isolates were found to harbor other carbapenemase genes $bla_{OXA-232}$, while none of the CR-hvKP isolates were found to harbor other carbapenemase genes. Among them, two CR-hvKP isolates harbored bla_{KPC-3}, two CR-hvKP isolates harbored bla_{NDM-1}, remarkably, all detected KPC-type genes and NDM-type genes of hv-CRKP isolates were bla_{KPC-2} and bla_{NDM-5}. In addition to carbapenemase genes, all isolates were screened using PCR for ESBL-encoding genes bla_{CTX}, bla_{SHV}, and bla_{TEM} (Fig. 5). Of the ESBL-producing CR-hvKP isolates, 10.5% (2/19) harbored the bla_{CTX}, 73.7% (14/19) harbored bla_{SHV}, and 26.3% (5/19) harbored bla_{TEM}. Among hv-CRKP isolates, the proportions of bla_{CTX}, bla_{SHV}, and bla_{TEM} were 63.3%, 81.1% and 46.7%, respectively. The plasmid-mediated fosfomycin resistance gene (*fosA*) was identified in almost all isolates in both groups, with a higher prevalence CR-hvKP (68.4%) than hv-CRKP (37.8%). Additionally, 68.4% of CR-hvKP carried the plasmid-mediated quinolone resistance gene *qnrS*, which was significantly higher carriage than hv-CRKP (37.8%). In contrast, the proportion of resistance genes in CR-hvKP and hv-CRKP showed significant differences.

According to whole-genome sequencing, several isolates carried rare antimicrobial resistance genes co-existing with virulence genes. One out of the *RmtF*-producing ST15-KL112 hv-CRKP FK3006 isolates co-existed the $bla_{OXA-232}$ and pLVPK-like virulence plasmid. Two CR-hvKP isolates, FK3048 and 1151, co-carried bla_{KPC-2}, bla_{NDM-1} and virulence plasmid.

SNP differences contributed to the observed variations in virulence and resistance phenotypes between isolates of different clusters in ST11-KL64 hv-CRKP

To explore the evolutionary difference with ST11-KL64 hv-CRKP, we constructed a phylogenomic tree based on the SNPs. Our analysis divided the 72 ST11-KL64 hv-CRKP isolates into 6 main cluster (A-F) (Fig. 6). Despite all isolates carried bla_{KPC-2}, cluster E and F were associated with high-level resistance to carbapenems (Meropenem, MIC>256) compared to the cluster A and C. Compared to cluster B and C, cluster D, E and F had a high-production of capsular polysaccharide and biofilm. The Quantitative siderophore assays showed that most bacterial isolates were able to produce high-level siderophore, except for cluster A and C.

Moreover, we found significant differences in virulence and resistance phenotypes even within the same cluster. Accordingly, we annotated a total of 843 genes among these ST11-KL64 hv-CRKP isolates, using FK3009 as the reference strain. We divided the isolates into two different groups based on differences in resistance and virulence phenotypes. The enrichment analysis results showed significant variations in many pathways between the two distinct phenotypic groups (Fig. 7). KEGG pathway enrichment analysis indicated that the citrate cycle (TCA cycle), glycolysis/gluconeogenesis, glutathione metabolism, two-component regulatory system, and folate metabolism pathways were the most enriched among the capsular polysaccharides differential groups (Fig. 7A). In addition to the significant differences in the biofilm synthesis pathway, expression of peptidoglycan biosynthesis and the quorum sensing system were also markedly pronounced within the biofilm differential groups (Fig. 7B). Genes of the siderophore differential groups were predominantly enriched in amino acid metabolism, quorum sensing systems, and ribonucleotide metabolism (Fig. 7C). The differentially resistant groups were primarily enriched in pathways related to antibiotic resistance and biofilm formation (Fig. 7D).

Discussion

With the widespread use of antibiotics and worldwide intensification of human-associated exchanges, hypervirulent and carbapenem-resistant *K.pneumoniae* has emerged in recent years[3, 8]. According to their evolutionary path, hypervirulent and carbapenem-resistant *K. pneumoniae* has been classified into three groups, with CR-hvKP and hv-CRKP being mainly prevalent worldwide. There was a high ST diversity across the CR-hvKP and hv-CRKP isolates. CR-hvKP was involved in a diverse range of STs and K-loci, and clone ST65, belonging to capsular serotypes KL2, and clone ST23, belonging to capsular serotypes K1, were the most common clones of hvKP isolates, respectively [11]. It should be noted that

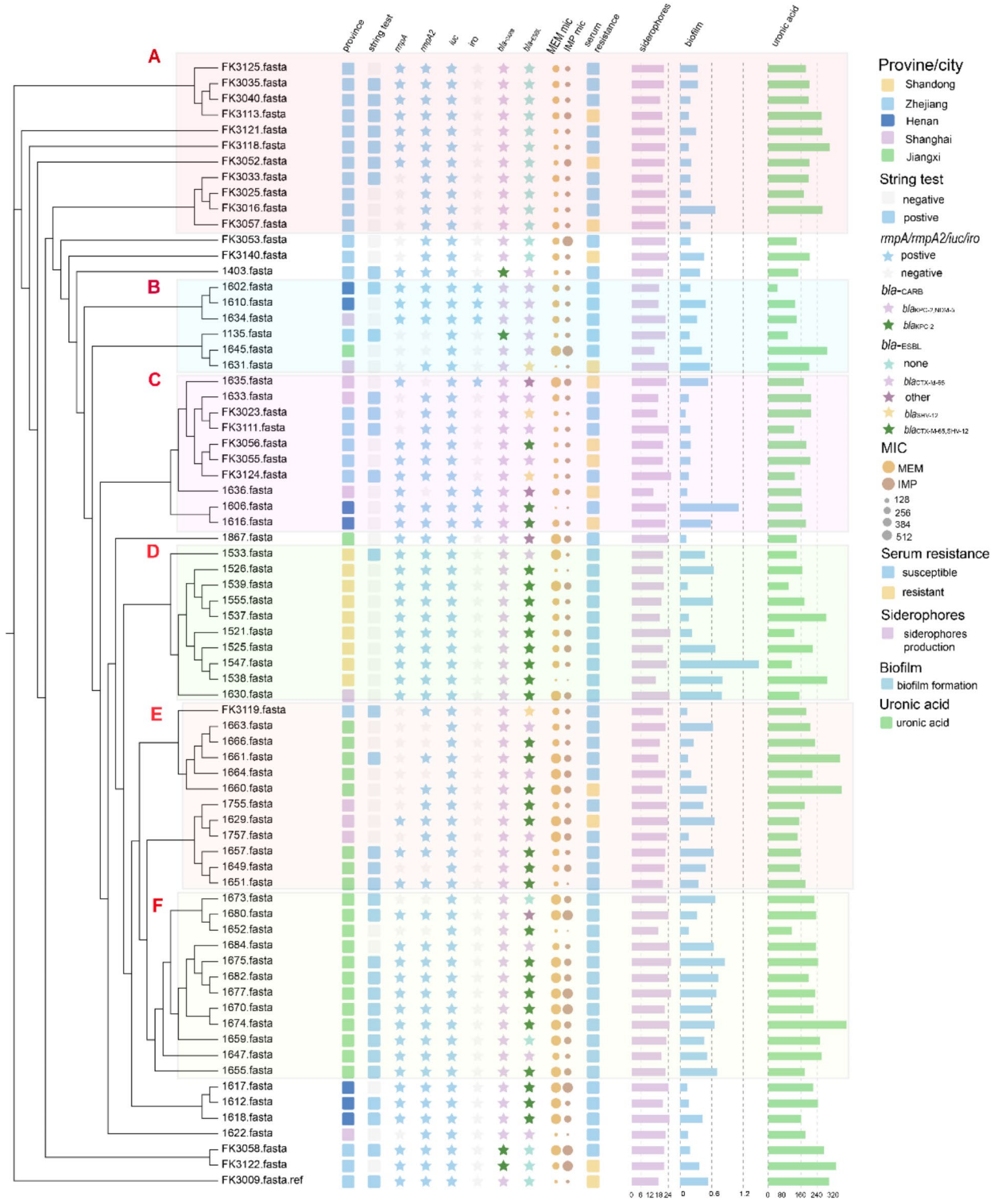

Fig. 6 The phylogenetic tree based on SNP matrix Evolutionary tree rooted on ST11-KL64 hv-CRKP FK3009 using SNP-based phylogenetic analysis of 72 ST11-KL64 hv-CRKP strains. Some of virulence and resistance genes detected were shown here. Aerobactin and salmochelin represent the *iuc*ABCD-*iutA* and *iroBCDN* gene clusters, respectively. The virulence phenotypic data were shown in colored bars. Circles represented MIC results

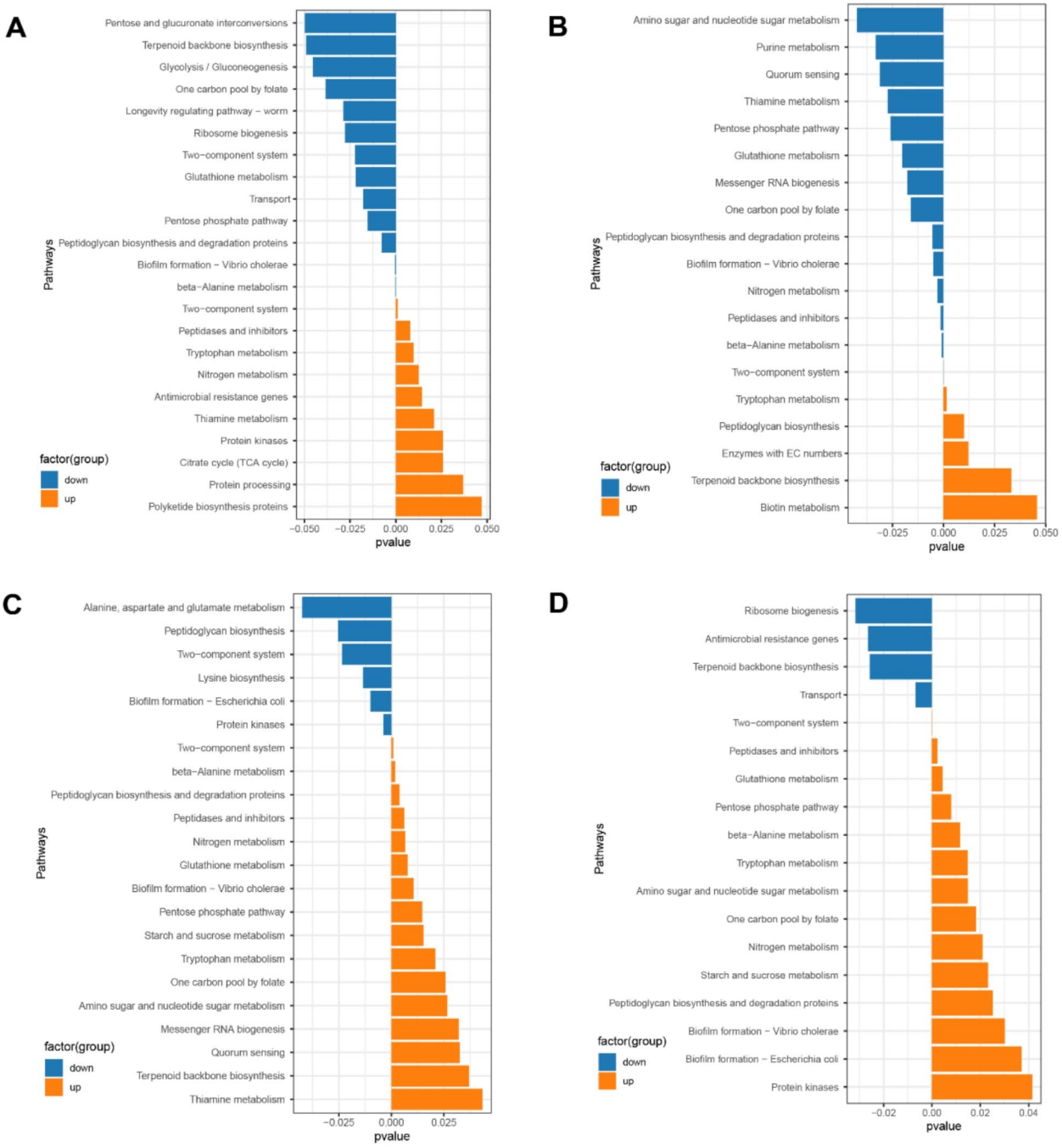

Fig. 7 KEGG pathway enrichment results The most significant KEGG pathways from the KEGG enrichment results are displayed. Significantly enriched pathways were determined by a p-value of less than 0.05. **A** KEGG analysis of differential genes between the high and low capsular groups. **B** KEGG analysis of differential genes between the high and low biofilm groups. **C** KEGG analysis of differential genes between the high and low siderophore groups. **D** KEGG analysis of differential genes between the high and low resistance to meropenem groups. The blue bar represents the mutant gene which was in low level phenotype strains. The orange bar represents the mutant gene which was in high level phenotype strains

hv-CRKP has been found to cause nosocomial infections and significant clonal hospital outbreaks. It was reported that KPC-producing ST11-hv-CRKP is the clonotype. Several studies have indicated that, in comparison to KL1/KL2 CR-hvKP, ST11 hv-CRKP has an enhanced virulence phenotype after acquiring pK2044-like virulence plasmids [8, 12]. Therefore, this study aimed to analyze the differences in virulence and resistance profiles among hv-CRKP and CR-hvKP, and revealed the highly

virulent and resistance phenotype of these ST11-KL64 CRKP isolates.

The horizontal transfer of transferrable resistant plasmid with high conjugation frequency may promote the emergence and dissemination of CR-hvKP. However, the ease of evolution of CR-hvKP did not correspond to our observations [13]. In this study, we comprehensively examined the true distribution of CR-hvKP and hv-CRKP isolates and observed that CR-hvKP strains were less prevalent than hv-CRKP isolates in hospitals and had a narrow resistance profile. Previous research found that hvKP produce a thick capsular on its surfaces to halt plasmid entry into bacteria [4]. Unlike CRKP, the high genomic homogeneity of hvKP posed a challenge for the acquisition of plasmids or integrative mobile elements [14–16]. Furthermore, the membrane protein OmpK35 has undergone a base insertion that leads to premature translation termination, reducing membrane permeability in cKP strains such as ST11[17]. On the other hand, OmpK36 incorporates a Loop3 containing glycine-aspartic acid (GD), which enhances the efficiency of membrane protein contraction compared to ST23-hvKP and is able to slow down the entry of carbapenems into bacteria [18]. In our previous works, we found that all almost KL1-hvKP carried a CRISPR-Cas3 system which significantly influenced the dissemination of F-type conjugative plasmid, while CG258 (ST11) lacked the CRISPR-Cas3 system [19].

Previous studies have observed that KL64 and KL47 belong to a large evolutionary branch, and KL47 was the evolutionary ancestor of KL64[12, 20, 21]. Our data revealed that the evolution of KL47 to KL64 is gradually becoming the mainstream trend, with ST11-KL47, the dominant subclone after 2015, being progressively replaced by ST11-KL64 in the CRKP ST11 lineage. These results are consistent with a recent study showing that the ST11-KL64 clone has replaced ST11-K47 due to the acquisition of a new fused plasmid. Previous studies have indicated a point mutation occurring in *recC* contributing to genetic variability, conferring greater recombination proficiency in KL64 compared to KL47[22]. In addition, horizontal gene transfer has been identified as another significant factor driving diversification in ST11, with KL64 exhibiting a notably higher abundance of mobile genetic elements (MGEs), including insertion sequences (ISs), plasmids and prophages, compared to KL47. Furthermore, there are differences in the carbapenem-resistant and virulence genes carried by CR-hvKP and hv-CRKP strains across different regions.

Although CR-hvKP carries carbapenemase enzymes, our study conducted an in-depth investigation into the level of carbapenem resistance in CR-hvKP and found that most of the CR-hvKP exhibited the intermediate or low level carbapenem resistance, suggesting low expression of these carbapenemase. Bacterial efflux pumps were considered the main mechanism of tigecycline resistance before it was discovered that mobile tigecycline resistance genes were located in plasmid-mediated bacterial resistance [23]. We found that, although the carriage rate of the genes related to various antibiotic efflux pumps, such as AcrAB-TolC and *oxqAB*, were high in CR-hvKP, the high frequency of tigecycline resistance correlates with the tigecycline resistance genes *tet*. The majority of strains carry bla_{KPC-2}, which is known for its complex and changeable genetic environment and can be carried by self-transmissible plasmids [24]. The mobilization of a pLVPK-like nonconjugative virulence plasmid into CRKP can be facilitated by a self-transferable IncF plasmid, as CPKP can maintain multiple plasmids with low fitness cost [25]. Further WGS analysis revealed that the presence of multiple resistance genes (*rmtB*, *fosA* and *qnsR*) on the typical IncF plasmid has led to high-level resistance to commonly used antibiotics in poultry, such as aminoglycoside, quinolone and fosfomycin. Our findings are consistent with the conciseness of antibiotic resistance.

We demonstrated that CR-hvKP strains carry an increased abundance of virulence genes, including *iroBCDN*, *rmpA*, and *rmpA2*. The regulatory gene *rmpA* regulates the biosynthesis of capsular polysaccharides, encoding a hypermucoviscous phenotype in the strains [26]. Deletion or mutation of *rmpA* may result in the loss or thinning of the capsule [27]. We further found several isolates with an intact *rmpA2* did not show a hypermucoviscosity phenotype, and some strains carrying the *rmpA2* mutations exhibited the hypermucoviscosity phenotype, implying that mechanisms other than *rmpA*/*rmpA2* could also mediate hypermucoviscous phenotype. hvKP exhibits four major virulence factors, namely, capsular polysaccharides, siderophores, fimbriae and lipopolysaccharides [28–30]. In our investigation, 19 isolates belonging to KL1/KL2 types, along with other CR-hvKP strains carrying resistant plasmids, exhibited the hypervirulent features. Previous studies found that different KL-type hvKP strains did not always maintain a high average virulence level after acquiring the bla_{KPC}-containing plasmid [25]. It is possible that the acquisition and expression of additional plasmids may impose a metabolic burden on hvKP, such that it is needed for the formation of capsule [31–33]. Interestingly, our virulence-associated studies showed CRKP strains had a hypervirulence phenotype after acquiring virulence factors, and virulence also exhibited substantial variation at the subspecies level. Notably, the ST11-KL64 strain fully exhibited the hypervirulent features and high-level carbapenems resistance (MIC 64-256 μg/mL). In contrast, the ST11-KL47 hv-CRKP exhibited significantly lower virulence compared to ST11-KL64 isolates and

NTUH-K2044 hypervirulent strain. Previous studies have observed that ST11-KL64 hv-CRKP had a remarkably higher 30-day mortality and sepsis/septic shock incidence and could rapidly lose and gain genes during interhospital transmission [8, 21]. Hence, the identified subclonal shift within CRKP-ST11 may affect not only control measures but also therapeutic strategies. Notably, there is a potential dissemination of ST 290 and ST15 clone secondary to the ST11 clones, and the true prevalence of these subtypes presents a significant clinical challenge.

The emergence of ST11-KL64 hv-CRKP, which causes high mortality rates in clinical patients, underscores the urgent need for investigations into the potential mechanism of resistance and virulence factors. Strains within the same clades also displayed varied levels of resistance and virulence. KEEG enrichment indicated that the SNP between virulence groups were mainly related to biofilm formation, beta-Alanine metabolism, peptidases and inhibitors and two-component system. Additionally, through KEEG enrichment analysis, we found that the transport, two-component system and peptidases and inhibitors were related to the function of resistance.

In this study, we investigated the molecular epidemiology of 109 non-repetitive CR-hvKP and hv-CRKP isolates from 11 centers in China, characterized the resistance and virulence phenotypes and molecular features, and observed the hv-CRKP strains were more prevalent than CR-hvKP strains in hospitals, exhibiting a high level of multi-resistance and virulence. Evolutionarily, the acquisition of virulence plasmids by CRKP strains is not common, but the coexistence of multiple resistance and virulence phenotype in CRKP was more transmitted. In addition, we found the ST11-KL64 hv-CPKP emerged as a dominated high-risk lineage, with enhanced MDR and a hypervirulent phenotype, requiring the most clinical attention. Our enrichment analysis, suggested that several pathways were associated with the virulence and resistance. Further investigations into the underlying mechanisms should be conducted in the future.

Supplementary Information

The online version contains supplementary material available at https://doi.org/10.1186/s12866-024-03614-9.

Supplementary Material 1

Acknowledgements

We thank the authority of NTUH-K2044 by Jin-Town Wang from National Taiwan University Hospital.

Author contributions

CW: conceptualization, data curation, formal analysis, methodology, and writing–original draft. YH and PZ: data curation, methodology, andwriting–original draft. HG and BW: methodology. HZ and JZ software and formal analysis. LW and YZ: conceptualization, project administration, and writing–review andediting. FY: conceptualization and writing–review and editing. Allauthors contributed to the article and approved the submitted version.

Funding

Not applicable.

Data availability

Sequence data that support the findings of this study have been deposited in NCBI with the BioSample accession code SAMN43180497-43180605.

Declarations

Ethics approval and consent to participate

This study was approved by the ethics committees of the First Affiliated Hospital of Wenzhou Medical University (WYYY-AEC-2022-025).

Consent for publication

Not applicable.

Competing interests

The authors declare no competing interests.

Author details

[1]Department of Endocrinology, The First Affiliated Hospital of Wenzhou Medical University, Wenzhou 325000, China
[2]Department of Laboratory Medicine, The First Affiliated Hospital of Wenzhou Medical University, Wenzhou 325000, China
[3]Department of Clinical Laboratory Medicine, Shanghai Pulmonary Hospital, Tongji University School of Medicine, Shanghai 200433, China
[4]Department of Respiratory Medicine, The First Affiliated Hospital of Wenzhou Medical University, Wenzhou 325000, China

Received: 1 August 2024 / Accepted: 28 October 2024
Published online: 11 November 2024

References

1. van Duin D, Doi Y. The global epidemiology of carbapenemase-producing Enterobacteriaceae. Virulence. 2017;8(4):460–9. https://doi.org/10.1080/21505594.2016.1222343.
2. Shon AS, Bajwa RP, Russo TA. Hypervirulent (hypermucoviscous) Klebsiella pneumoniae: a new and dangerous breed. Virulence. 2013;4(2):107–18. https://doi.org/10.4161/viru.22718.
3. Yang X, Dong N, Chan EW, Zhang R, Chen S. Carbapenem resistance-encoding and Virulence-encoding conjugative plasmids in Klebsiella pneumoniae. Trends Microbiol. 2021;29(1):65–83. https://doi.org/10.1016/j.tim.2020.04.012.
4. Cejas D, Fernandez Canigia L, Rincon Cruz G, Elena AX, Maldonado I, Gutkind GO, et al. First isolate of KPC-2-producing Klebsiella pneumonaie sequence type 23 from the Americas. J Clin Microbiol. 2014;52(9):3483–5. https://doi.org/10.1128/JCM.00726-14.
5. Dong N, Liu L, Zhang R, Chen K, Xie M, Chan EWC, et al. An IncR plasmid harbored by a hypervirulent carbapenem-resistant Klebsiella pneumoniae strain possesses five tandem repeats of the bla(KPC-2)::NTE(KPC)-Id fragment. Antimicrob Agents Chemother. 2019;63(3). https://doi.org/10.1128/AAC.01775-18.
6. Xu M, Fu Y, Fang Y, Xu H, Kong H, Liu Y, et al. High prevalence of KPC-2-producing hypervirulent Klebsiella pneumoniae causing meningitis in Eastern China. Infect Drug Resist. 2019;12:641–53. https://doi.org/10.2147/IDR.S191892.
7. Xie M, Chen K, Ye L, Yang X, Xu Q, Yang C, et al. Conjugation of Virulence plasmid in clinical Klebsiella pneumoniae strains through formation of a fusion plasmid. Adv Biosyst. 2020;4(4):e1900239. https://doi.org/10.1002/adbi.201900239.
8. Gu D, Dong N, Zheng Z, Lin D, Huang M, Wang L, et al. A fatal outbreak of ST11 carbapenem-resistant hypervirulent Klebsiella pneumoniae in a Chinese hospital: a molecular epidemiological study. Lancet Infect Dis. 2018;18(1):37–46. https://doi.org/10.1016/S1473-3099(17)30489-9.
9. Shelenkov A, Mikhaylova Y, Yanushevich Y, Samoilov A, Petrova L, Fomina V, et al. Molecular typing, characterization of antimicrobial resistance, Virulence profiling and analysis of whole-genome sequence of clinical Klebsiella

pneumoniae isolates. Antibiotics (Basel). 2020;9(5). https://doi.org/10.3390/antibiotics9050261.
10. Zhou Y, Wu C, Wang B, Xu Y, Zhao H, Guo Y, et al. Characterization difference of typical KL1, KL2 and ST11-KL64 hypervirulent and carbapenem-resistant Klebsiella pneumoniae. Drug Resist Updat. 2023;67:100918. https://doi.org/10.1016/j.drup.2023.100918.
11. Russo TA, Marr CM. Hypervirulent Klebsiella pneumoniae. Clin Microbiol Rev. 2019;32(3). https://doi.org/10.1128/CMR.00001-19.
12. Yang Q, Jia X, Zhou M, Zhang H, Yang W, Kudinha T, et al. Emergence of ST11-K47 and ST11-K64 hypervirulent carbapenem-resistant Klebsiella pneumoniae in bacterial liver abscesses from China: a molecular, biological, and epidemiological study. Emerg Microbes Infect. 2020;9(1):320–31. https://doi.org/10.1080/22221751.2020.1721334.
13. Zhang Y, Jin L, Ouyang P, Wang Q, Wang R, Wang J, et al. Evolution of hypervirulence in carbapenem-resistant Klebsiella pneumoniae in China: a multicentre, molecular epidemiological analysis. J Antimicrob Chemother. 2020;75(2):327–36. https://doi.org/10.1093/jac/dkz446.
14. Campos MA, Vargas MA, Regueiro V, Llompart CM, Alberti S, Bengoechea JA. Capsule polysaccharide mediates bacterial resistance to antimicrobial peptides. Infect Immun. 2004;72(12):7107–14. https://doi.org/10.1128/IAI.72.12.7107-7114.2004.
15. Wyres KL, Wick RR, Judd LM, Froumine R, Tokolyi A, Gorrie CL, et al. Distinct evolutionary dynamics of horizontal gene transfer in drug resistant and virulent clones of Klebsiella pneumoniae. PLoS Genet. 2019;15(4):e1008114. https://doi.org/10.1371/journal.pgen.1008114.
16. Durao P, Balbontin R, Gordo I. Evolutionary mechanisms shaping the mMaintenance of antibiotic resistance. Trends Microbiol. 2018;26(8):677–91. https://doi.org/10.1016/j.tim.2018.01.005.
17. Tsai YK, Fung CP, Lin JC, Chen JH, Chang FY, Chen TL, et al. Klebsiella pneumoniae outer membrane porins OmpK35 and OmpK36 play roles in both antimicrobial resistance and virulence. Antimicrob Agents Chemother. 2011;55(4):1485–93. https://doi.org/10.1128/AAC.01275-10.
18. David S, Wong JLC, Sanchez-Garrido J, Kwong HS, Low WW, Morecchiato F, et al. Widespread emergence of OmpK36 loop 3 insertions among multidrug-resistant clones of Klebsiella pneumoniae. PLoS Pathog. 2022;18(7):e1010334. https://doi.org/10.1371/journal.ppat.1010334.
19. Zhou Y, Yang Y, Li X, Tian D, Ai W, Wang W, et al. Exploiting a conjugative endogenous CRISPR-Cas3 system to tackle multidrug-resistant Klebsiella pneumoniae. EBioMedicine. 2023;88:104445. https://doi.org/10.1016/j.ebiom.2023.104445.
20. Liao W, Liu Y, Zhang W. Virulence evolution, molecular mechanisms of resistance and prevalence of ST11 carbapenem-resistant Klebsiella pneumoniae in China: A review over the last 10 years. J Glob Antimicrob Resist. 2020;23:174–80. https://doi.org/10.1016/j.jgar.2020.09.004.
21. Zhou K, Xiao T, David S, Wang Q, Zhou Y, Guo L, et al. Novel subclone of carbapenem-resistant Klebsiella pneumoniae sequence type 11 with e Virulence and transmissibility, China. Emerg Infect Dis. 2020;26(2):289–97. https://doi.org/10.3201/eid2602.190594.
22. Zhou K, Xue CX, Xu T, Shen P, Wei S, Wyres KL, et al. A point mutation in recC associated with subclonal replacement of carbapenem-resistant Klebsiella pneumoniae ST11 in China. Nat Commun. 2023;14(1):2464. https://doi.org/10.1038/s41467-023-38061-z.
23. Rajendran R, Quinn RF, Murray C, McCulloch E, Williams C, Ramage G. Efflux pumps may play a role in tigecycline resistance in Burkholderia species. Int J Antimicrob Agents. 2010;36(2):151–4. https://doi.org/10.1016/j.ijantimicag.2010.03.009.
24. Carattoli A, Zankari E, Garcia-Fernandez A, Voldby Larsen M, Lund O, Villa L, et al. In silico detection and typing of plasmids using plasmid finder and plasmid multilocus sequence typing. Antimicrob Agents Chemother. 2014;58(7):3895–903. https://doi.org/10.1128/AAC.02412-14.
25. Tian D, Liu X, Chen W, Zhou Y, Hu D, Wang W, et al. Prevalence of hypervirulent and carbapenem-resistant Klebsiella pneumoniae under divergent evolutionary patterns. Emerg Microbes Infect. 2022;11(1):1936–49. https://doi.org/10.1080/22221751.2022.2103454.
26. Hsu CR, Lin TL, Chen YC, Chou HC, Wang JT. The role of Klebsiella pneumoniae rmpA in capsular polysaccharide synthesis and virulence revisited. Microbiology (Reading). 2011;157(Pt 12):3446–57. https://doi.org/10.1099/mic.0.050336-0.
27. Cheng HY, Chen YS, Wu CY, Chang HY, Lai YC, Peng HL. RmpA regulation of capsular polysaccharide biosynthesis in Klebsiella pneumoniae CG43. J Bacteriol. 2010;192(12):3144–58. https://doi.org/10.1128/JB.00031-10.
28. Struve C, Roe CC, Stegger M, Stahlhut SG, Hansen DS, Engelthaler DM, et al. Mapping the evolution of hypervirulent Klebsiella pneumoniae. mBio. 2015;6(4):e00630. https://doi.org/10.1128/mBio.00630-15.
29. Russo TA, Olson R, Fang CT, Stoesser N, Miller M, MacDonald U, et al. Identification of biomarkers for differentiation of hypervirulent Klebsiella pneumoniae from classical K. pneumoniae. J Clin Microbiol. 2018;56(9). https://doi.org/10.1128/JCM.00776-18.
30. Puorger C, Vetsch M, Wider G, Glockshuber R. Structure, folding and stability of FimA, the main structural subunit of type 1 pili from uropathogenic Escherichia coli strains. J Mol Biol. 2011;412(3):520–35. https://doi.org/10.1016/j.jmb.2011.07.044.
31. Buckner MMC, Saw HTH, Osagie RN, McNally A, Ricci V, Wand ME, et al. Clinically relevant plasmid-host interactions indicate that transcriptional and not genomic modifications Ameliorate fitness costs of Klebsiella pneumoniae carbapenemasec-carrying plasmids. mBio. 2018;9(2). https://doi.org/10.1128/mBio.02303-17.
32. Mike LA, Stark AJ, Forsyth VS, Vornhagen J, Smith SN, Bachman MA, et al. A systematic analysis of hypermucoviscosity and capsule reveals distinct and overlapping genes that impact Klebsiella pneumoniae fitness. PLoS Pathog. 2021;17(3):e1009376. https://doi.org/10.1371/journal.ppat.1009376.
33. Whitfield C, Wear SS, Sande C. Assembly of bacterial capsular polysaccharides and exopolysaccharides. Annu Rev Microbiol. 2020;74:521–43. https://doi.org/10.1146/annurev-micro-011420-075607.

Publisher's note